

## Dipolar interactions in two- and three-dimensional magnetic nanoparticle arrays

Pankaj Poddar, Tamar Telem-Shafir, Tcipi Fried, and Gil Markovich\*

*School of Chemistry, Tel Aviv University, Tel Aviv 69978, Israel*

(Received 3 May 2002; published 8 August 2002)

Uniform, organically functionalized, 8.5-nm-diameter nanocrystals of  $\text{Fe}_3\text{O}_4$  were synthesized and assembled into close-packed monolayer as well as multilayer arrays using the Langmuir-Blodgett technique. The ac and dc magnetic susceptibility measurements on arrays in comparison with isolated particles indicate strong dipolar interactions and a spin-glass-like slowing down of relaxation times. Differences in magnetic characteristics between monolayer to multilayer arrays were observed, such as larger remanent magnetization and a higher blocking temperature in the two-dimensional system.

DOI: 10.1103/PhysRevB.66.060403

PACS number(s): 75.75.+a, 75.20.-g, 81.07.Bc, 75.50.Tt

Ensembles of magnetic nanoparticles in various forms were at the focus of scientific interest since the days of Néel<sup>1</sup> and Brown,<sup>2</sup> who developed the theory for magnetization relaxation for noninteracting single-domain ferromagnetic and ferrimagnetic particles. Magnetization studies of frozen ferrofluids explored the differences between isolated and interacting particle behaviors by changing their concentration in the carrier liquid.<sup>3,4</sup> Since these single-domain particles are characterized by coherent activated rotation or by switching of the individual atomic magnetic moments in a particle,<sup>5</sup> each particle behaves as a large magnetic dipole with its orientation fluctuating according to the temperature and anisotropy of the particle. The collection of interacting magnetic dipoles served, both experimentally<sup>4,6,7</sup> and theoretically<sup>8,9</sup> as a model system to observe interesting cooperative physical phenomena. The most intensively studied was probably the spin-glass-like phase transition that was expected to occur in a collection of strongly interacting magnetic dipoles by lowering the thermal energy below the dipolar interaction energy.<sup>4,10</sup>

More recent preparations of magnetic nanocrystals produced by chemical synthesis routes<sup>11-15</sup> could potentially advance the studies of interacting magnetic particles. The better uniformity and control over particle size and interparticle separation may resolve various effects previously obscured by the inhomogeneous broadening that made the analysis of data obtained from ferrofluid measurements difficult. By modifying interparticle separation through an exchange of the organic surfactants protecting the nanocrystals, and by controlling the packing geometry or the particle sizes produced at the synthesis, one would hope to tune interparticle interactions between weak and strong dipolar interactions. The strength of dipolar interactions is relative to the individual particle anisotropy energy  $E_a$  arising either from bulk crystalline anisotropy ( $KV$ , where  $K$  is anisotropy constant and  $V$  the particle volume) or particle's shape and surface anisotropy.

In the case of weak interparticle interactions, the magnetic behavior as a function of temperature was typically approximated as individual particle magnetization freezing at the blocking temperature ( $T_b$ ) due to the anisotropy energy barrier with a correction term contributed by dipolar interactions. In a weakly interacting ferrofluid sample the freezing of magnetic moments has been described as isolated block-

ing events of particles with decreasing temperature according to particle anisotropy and inhomogeneous dipolar interaction distributions.<sup>16</sup> For a random array of strongly interaction particles, a collective disordered magnetization freezing was deduced from experimental data,<sup>17</sup> similar to spin-glass transitions studied in various diluted magnetic metal alloys.<sup>18</sup>

Although spectacular uniformity in particle size has recently been obtained for Co,<sup>11</sup> PtFe,<sup>19</sup> and  $\text{Fe}_2\text{O}_3$  (Ref. 14) magnetic nanoparticle preparations, the techniques used to prepare particle arrays, such as drop casting and similar solvent evaporation schemes,<sup>11,20</sup> lack the ability to control the packing uniformity of the nanoparticles on a macroscopic scale. In addition, it was found that for Co particles, for example, the apparent size uniformity did not result in an equivalent magnetic uniformity due to crystalline defects, which led to varying anisotropies and saturation magnetization values between the nanocrystals.<sup>21</sup>

In this paper, we report on magnetization studies of two-dimensional (2D) close-packed arrays of fatty acid coated  $\text{Fe}_3\text{O}_4$  nanocrystals, of microscopic uniformity extending to the cm scale, which were formed using the Langmuir-Blodgett (LB) technique. Similar close-packed arrays were recently used for magnetotransport<sup>22</sup> and magneto-optical experiments.<sup>23</sup> By stacking several LB monolayers quasi-three-dimensional (Q3D) arrays were produced. Isolated particle samples were obtained by diluting the particles in dodecane.

The preparation of the arrays is described in detail elsewhere.<sup>24</sup> The  $\text{Fe}_3\text{O}_4$  nanocrystals were formed by mixing  $\text{Fe}^{2+}$  and  $\text{Fe}^{3+}$  (1:2 molar ratio) in an aqueous medium and treating with ammonia at around 80 °C under inert atmosphere, followed by coating the resulting nanoparticles with oleic acid and neutralizing their surface charge. The coated particles, typically in the size range of 3–10 nm, were transferred to heptane and separated by size selective precipitation into samples of varying average size and size distribution. LB films were prepared by depositing the heptane solution at the air-water interface and compressing two dimensionally to form close-packed monolayers.

The monolayer used for this study was deposited on a carbon-coated copper grid to characterize its uniformity, size distribution, and interparticle separation using transmission electron microscopy (TEM). The TEM image revealed that the monolayer was close packed with particles arranged in a

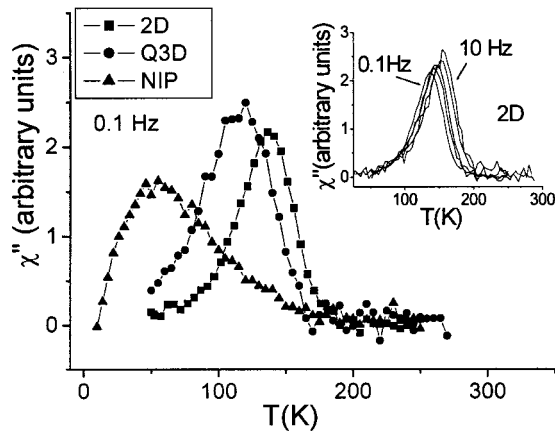


FIG. 1. Imaginary component of 0.1-Hz ZFC ac susceptibility plotted against temperature. The inset shows the shift in  $T_b$  with increasing ac frequency for the 2D sample.

short-range ordered hexagonal network. The particles were nearly spherical in shape with an average size of  $8.5 \pm 1.4$  nm, although slight shape anisotropy could be observed in many of the particles. The average interparticle separation due to the surfactant coating was 2.4 nm. The layers in this form were stable at ambient conditions as well as at elevated temperature (as high as 300 °C). For magnetic property measurements, monolayers were deposited from the air-water interface onto fused-silica substrates: a single monolayer (2D) and five monolayers stacked one on top of another (Q3D) were deposited. The surface topography of the monolayer samples was imaged by tapping-mode atomic force microscopy, confirming the presence of a monolayer over >90% of the substrate area. The rest of the surface was covered by bilayer domains. A dilute solution of nearly isolated particles (NIP's) dispersed in dodecane with excess of oleic acid to minimize agglomeration of the particles was prepared from the same batch of particles, as a reference of non-interacting particles.

In-plane dc magnetization curves as well as ac susceptibility measurements as function of temperature and frequency were performed using a superconducting quantum interference device magnetometer (Quantum Design XL-5). Data were carefully corrected for substrate or solvent background contributions. The NIP sample was filled in gelatin capsules and inserted in the magnetometer at 250 K to allow the dodecane to freeze with the particles' easy-axes distributed randomly, as in the case of the monolayers.

For zero-field-cooled (ZFC) ac magnetic susceptibility measurements the samples were cooled down to 4 K under zero external field, and the complex susceptibility was measured with heating the sample at a frequency range of 0.1–100 Hz and a field amplitude of 4 Oe for both layered and NIP samples. Figure 1 captures the essential differences in the imaginary susceptibility component vs temperature curves between the samples measured at 0.1 Hz. The peak in susceptibility for the 2D sample appears at a temperature higher than the peak of the NIP sample by a factor of 2.5 and, remarkably, higher than the peak of the Q3D sample. In addition, the NIP curve is relatively broader and drops to zero close to  $T=0$  K. On the other hand, the 2D curve is

narrower and drops to zero susceptibility at a much higher temperature ( $\sim 50$  K).

The inset in Fig. 1 shows that the peak of the imaginary component of the susceptibility, for the 2D sample, shifts to higher temperatures with increasing frequency, as typically observed for a collection of superparamagnetic particles.<sup>4,6</sup> The peak in the ZFC curves of isolated superparamagnetic particles is associated with  $T_b$ , which depends on the time scale of the experiment through the expression:  $\tau = \tau_0 \exp(E_a/k_B T)$  where  $k_B$  is the Boltzmann constant,  $\tau$  is the characteristic observation time,  $\tau_0$  is the “attempt time,” and  $E_a$  is the anisotropy energy. The anisotropy may come from volume anisotropy as well as surface and shape anisotropies. The distribution of the anisotropy energies is reflected in the broader peak of the NIP curve in Fig. 1. The narrowing of the 2D curve together with its large shift to higher temperatures is clear evidence of the existence of relatively strong dipolar interactions between the magnetic moments of the individual particles. This interaction energy thus appears to be larger than the isolated particle anisotropy energy but not much higher than room temperature thermal energy ( $k_B T$ ), as no hysteresis appears in the room temperature magnetization curve of the 2D sample. Therefore it is concluded that the magnetic moment freezing (blocking) behavior of the 2D and Q3D samples is dominated by interparticle dipolar interactions unlike the freezing of the NIP magnetic moments which is dominated by individual (or small aggregate) particle anisotropy.

The real part of the susceptibility fitted the Curie-Weiss law  $\chi(T) = C/(T - T_c)$  well above  $T_b$ , where  $C$  is a constant, and  $T_c$  is the critical temperature related to interparticle interactions. For the NIP sample  $T_c = 8 \pm 2$  K and does not change with the time-scale of measurement, i.e., the particles are effectively noninteracting.

According to Néel's theory of superparamagnetism,<sup>1,25</sup>  $T_b$  of a single domain particle is related to the particle volume ( $V$ ) and the anisotropy constant ( $K$ ) through  $25k_B T_b = KV$ . Using this relation for the NIP sample with  $T_b = 62$  K obtained from the ac results at 1 Hz,  $K$  was estimated to be  $7 \times 10^4$  J/m<sup>3</sup>. For the Fe<sub>3</sub>O<sub>4</sub> nanoparticles in ferrofluid form,<sup>3</sup> the value of  $K$  was reported to be  $2.3 \times 10^3$  J/m<sup>3</sup>. The upper inset of Fig. 2 shows a plot of the relaxation time  $\tau = (2\pi f)^{-1}$  vs  $1/T_b$  for the NIP sample. This curve fitted the Néel-Brown model,  $\tau = \tau_0 \exp(KV/k_B T)$ , reasonably well, and the values of  $K = 5 \times 10^4$  J/m<sup>3</sup> and  $\tau_0 = 4 \times 10^{-9}$  sec were extracted. Differences between bulk anisotropy values extracted from various experiments probably originate in variations of shape and surface anisotropies between the samples.

$T_b$  was higher in the array samples and its variation with  $\tau$  was weaker. These curves could not be fitted with the Néel-Brown model. To investigate the dynamics of the strongly interacting systems (2D and Q3D), we have studied the dependence of the relaxation time  $(2\pi f)^{-1}$  on  $T_b$ . According to previous work on spin-glass systems several functional forms may fit the rate of slowing down with decreasing temperature. Fits to a critical scaling power law<sup>4</sup> and to a modified exponential dependence (Vogel-Fulcher) were both attempted.

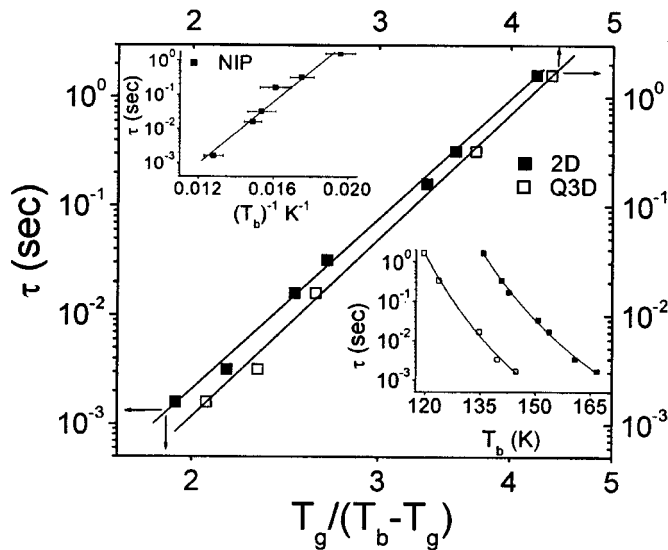


FIG. 2. Relaxation time plotted as a function of  $T_g/(T_b - T_g)$  for the array samples according to the dynamic scaling law. The lower inset shows a fit of 2D and Q3D data to the Vogel-Fulcher law. The upper inset shows the fit to the Néel-Brown model for the NIP sample. The points are experimental data and the solid lines are the fitted curves.

The scaling law expression  $\tau = \tau^* [T_g/(T_b - T_g)]^{z\nu}$  describes the divergence of  $\tau$  towards the glass transition temperature,  $T_g$ .  $\tau^*$  is a prefactor and  $z\nu$  is the critical exponent composed of a static part,  $\nu$ , and a dynamic part,  $z$ . As shown in Fig. 2, the data points for the two array samples fitted well this functional form. For both 2D and Q3D samples a critical exponent of  $9 \pm 1$  was obtained, which is within the error bar of the value obtained by Djurberg *et al.*<sup>4</sup> for Fe-C particles ( $11 \pm 3$ ) and a value of 8 obtained for  $\text{Co}_{80}\text{Fe}_{20}$  particles.<sup>26</sup> The glass transition temperature obtained for the 2D sample,  $110 \pm 9$  K, was higher than the transition temperature fitting the Q3D data,  $97 \pm 14$  K, and the prefactors were both in the  $10^{-6}$ -sec range.

In the lower inset of Fig. 2, we have successfully fitted the same data to the Vogel-Fulcher law:  $\tau = \tau_0 \exp[E_a/\kappa_B(T - T_0)]$ , where  $E_a$  is the activation energy and  $T_0$  is the transition temperature. Fitted  $\tau_0$  values for both 2D and Q3D samples were of the order expected for the high-temperature limit:  $8(\pm 3) \times 10^{-10}$  and  $2.5(\pm 2) \times 10^{-10}$  sec, respectively. The values of  $T_0$  for the 2D and Q3D samples were 71 and 64 K.

Figure 3 plots the real susceptibility component vs temperature at various frequencies for the 2D and NIP samples. A sharper magnetization freezing is again observed for the 2D case. The NIP susceptibility curves increase with a relatively large slope already at temperatures of few K, while the 2D susceptibility curves start increasing significantly only above 50 K. This behavior is another manifestation of the fundamental difference in the low temperature magnetization dynamics between the two types of samples. The isolated particle sample has a finite switching probability at low temperatures, which gives rise to the fast rising curves close to  $T=0$ . The 2D sample, on the other hand, freezes completely at a finite temperature,<sup>27</sup> where at all time scales the suscep-

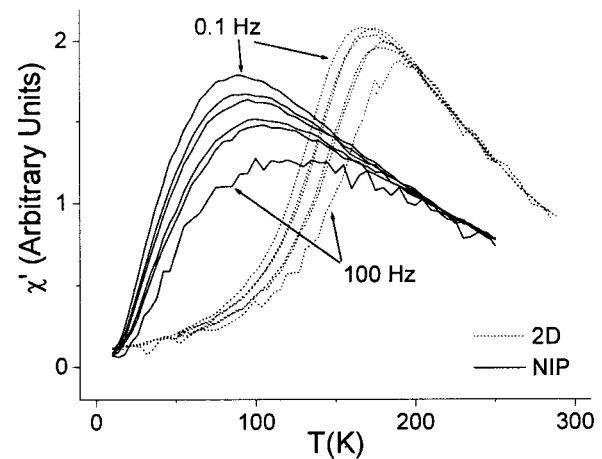


FIG. 3. Real component of the ac susceptibility vs temperature at different frequencies for the 2D and NIP samples.

tibility approaches zero. This type of apparently collective freezing (determined by dipolar energy barrier) is similar to spin freezing in spin glasses.

The increase in blocking temperature from Q3D to 2D samples can be explained in the following way: At  $T < T_b$  the particle moments are frozen according to their energetically favorable directions dominated by the dipolar interaction. For the 2D sample, due to strong demagnetizing fields for out-of-plane moments, the particles' moments should be frozen in the plane of the substrate. The lowest energy paths for reversing the in-plane magnetic moments are through in-plane rotation, where barriers are relatively large. On the other hand, due to the interlayer dipolar interactions, the Q3D sample should have a large fraction of particles with a significant out of plane magnetization component. Consequently, the moments at the Q3D sample should have lower barriers for rotation.

dc magnetization measurements revealed interesting differences between the three samples. The magnetization curves were measured at varying temperatures, showing zero coercivity ( $H_c$ ) above  $T_b$  and the onset of magnetic hysteresis around  $T_b$ . Figure 4 displays the low-temperature (10

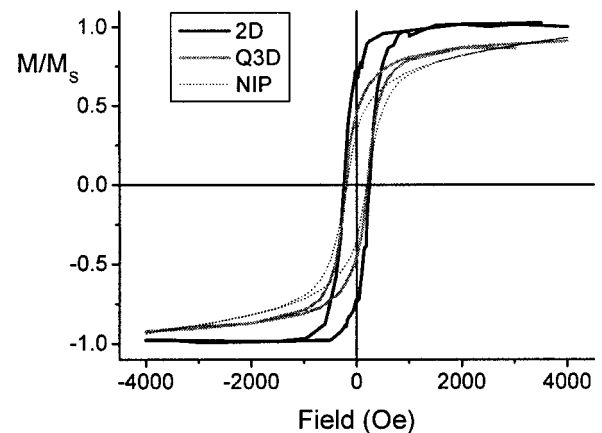


FIG. 4. Magnetic hysteresis curves for the three samples measured at 10 K. The magnetization is normalized to the saturation magnetization  $M_s$ .

K) normalized magnetization curves of the three samples. It can be seen that  $H_c$  is approximately constant for all the samples while the remanent to saturation magnetization ratio ( $M_r/M_s$ ) is significantly larger for the 2D sample in comparison to the Q3D and NIP samples, being 0.7 for the 2D sample, 0.45 for the Q3D sample, and 0.33 for the NIP sample. Another significant difference is the occurrence of saturation for the 2D curve at relatively lower magnetic field (2000 Oe) compared with the NIP and Q3D curves. The behavior of the dc magnetization curve for the 2D sample conforms to the picture obtained from the ac measurements: the larger barrier for in-plane magnetization rotation causes the observed large remanent magnetization. The low saturation field can be explained<sup>12</sup> by the lowest energy configuration of the 2D sample, which has all the moments aligned in plane. Thus, after overcoming the dipolar rotation barrier by the external field, the system easily finds the local energy minimum with opposite magnetization. In the Q3D case, because of the out of plane magnetization components, the external field (in plane) has to act against the dipolar interaction to bring the individual magnetic moments into an in-plane configuration. A similar argument can be used for the NIP sample where the individual particle moments are blocked with random orientation in space and the external field has to act against the anisotropy energy barrier to align the moments in the field direction.

In summary, we have presented distinct differences in the magnetic behavior of magnetic nanocrystal assemblies rang-

ing from isolated superparamagnetic nanocrystals via a 2D array to a Q3D array. While changing the dimensionality of the arrays from 2D to 3D, the stabilization of the out-of-plane component of the dipolar interaction leads to a lowering of blocking temperatures and reduces the low-temperature remanent magnetization. The strong dipolar interactions dominate the magnetic properties of the arrays over the anisotropy of the individual particles. The magnetic moments of the particles arranged in a closed-packed hexagonal network behave similarly to spin glasses at low temperatures, and their relaxation time distribution fits either a power law which includes a glass transition temperature  $T_g$  or an exponential slowing down to a lower transition temperature.

Apart from a difference in the transition temperature obtained from this fit, both 2D and Q3D data yield similar critical exponents and attempt frequencies. This behavior of the dipolar coupled magnetic nanoparticle arrays is probably different from structurally disordered, exchange-coupled spin glasses where smaller critical exponents were found and stronger dimensionality effects are expected for the transition temperatures.

This work was supported by The Israel Science Foundation Grant No. 152/99 and by the Nanoscience and Nanotechnology project at Tel Aviv University.

\*Corresponding author. Email address: gilmar@post.tau.ac.il

<sup>1</sup>L. Néel, *Ann. Geofis.* **5**, 99 (1949).

<sup>2</sup>W. F. Brown, Jr., *Phys. Rev.* **130**, 1677 (1963).

<sup>3</sup>W. Luo, S. Nagel, T. F. Rosenbaum, and R. E. Rosensweig, *Phys. Rev. Lett.* **67**, 2721 (1991).

<sup>4</sup>C. Djurberg, P. Svedlindh, P. Nordblad, M. F. Hansen, F. Bodker, and S. Morup, *Phys. Rev. Lett.* **79**, 5154 (1997).

<sup>5</sup>W. Wernsdorfer, E. Bonet Orozco, K. Hasselbach, A. Benoit, B. Barbara, N. Demoncy, A. Loiseau, H. Pascard, and D. Maily, *Phys. Rev. Lett.* **78**, 1791 (1997).

<sup>6</sup>J. L. Dormann, D. Fiorani, R. Cherkaoui, E. Tronc, F. Lucari, F. D'Orazio, L. Spinu, M. Noguez, H. Kachkachi, and J. P. Jolivet, *J. Magn. Magn. Mater.* **203**, 23 (1999).

<sup>7</sup>G. A. Held, G. Grinstein, H. Doyle, S. Sun, and C. B. Murray, *Phys. Rev. B* **64**, 012408 (2001).

<sup>8</sup>J. O. Andersson, C. Djurberg, T. Jonsson, P. Svedlindh, and P. Nordblad, *Phys. Rev. B* **56**, 13 983 (1997).

<sup>9</sup>V. Russier, *J. Appl. Phys.* **89**, 1287 (2001).

<sup>10</sup>J. L. Dormann, D. Fiorani, R. Cherkaoui, L. Spinu, F. Lucari, F. D'Orazio, M. Noguez, E. Tronc, J. P. Jolivet, and A. Garcia, *Nanostruct. Mater.* **12**, 757 (1999).

<sup>11</sup>S. Sun and C. B. Murray, *J. Appl. Phys.* **85**, 4325 (1999).

<sup>12</sup>C. Petit, A. Taleb, and M. P. Pileni, *J. Phys. Chem. B* **103**, 1805 (1999).

<sup>13</sup>E. E. Carpenter, C. T. Seip, and C. J. O'Connor, *J. Appl. Phys.* **85**, 5184 (1999).

<sup>14</sup>T. Hyeon, S. S. Lee, J. Park, Y. Chung, and H. Bin Na, *J. Am. Chem. Soc.* **123**, 12798 (2001).

<sup>15</sup>J. Rockenberger, E. C. Scher, and A. P. Alivisatos, *J. Am. Chem. Soc.* **121**, 11595 (1999).

<sup>16</sup>T. Jonsson, J. Mattsson, P. Nordblad, and P. Svedlindh, *J. Magn. Magn. Mater.* **168**, 269 (1997).

<sup>17</sup>T. Jonsson, P. Svedlindh, and M. F. Hansen, *Phys. Rev. Lett.* **81**, 3976 (1998).

<sup>18</sup>K. H. Fischer and J. A. Hertz, *Spin Glasses* (Cambridge University Press, Cambridge, 1991).

<sup>19</sup>S. Sun, C. B. Murray, D. Weller, L. Folks, and A. Moser, *Science* **287**, 1989 (2000).

<sup>20</sup>V. Russier, C. Petit, J. Legrand, and M. P. Pileni, *Appl. Surf. Sci.* **164**, 193 (2000).

<sup>21</sup>M. R. Diehl, J.-Y. Yu, J. R. Heath, G. A. Held, H. Doyle, S. Sun, and C. B. Murray, *J. Phys. Chem. B* **105**, 7913 (2001).

<sup>22</sup>P. Poddar, T. Fried, and G. Markovich, *Phys. Rev. B* **65**, 172405 (2002).

<sup>23</sup>G. Shemer and G. Markovich (unpublished).

<sup>24</sup>T. Fried, G. Shemer, and G. Markovich, *Adv. Mater.* **13**, 1158 (2001).

<sup>25</sup>A. T. Ngo, P. Bonville, and M. P. Pileni, *J. Appl. Phys.* **89**, 3370 (2001).

<sup>26</sup>S. Sahoo, O. Petravic, Ch. Binek, W. Kleemann, J. B. Sousa, S. Cardoso, and P. P. Freitas, *Phys. Rev. B* **65**, 134406 (2002).

<sup>27</sup>T. Jonsson, J. Mattsson, C. Djurberg, F. A. Khan, P. Nordblad, and P. Svedlindh, *Phys. Rev. Lett.* **75**, 4138 (1995).